




Broadband and compact folded substrate integrated waveguide phase shifter and its application to 180° directional coupler

Fang Zhu , Xin Zhao, Junhao Sheng and Guo Qing Luo

Key Laboratory of RF Circuits and Systems of Ministry of Education, School of Electronics and Information, Hangzhou Dianzi University, Hangzhou 310018, China

Research Paper

Cite this article: Zhu F, Zhao X, Sheng J, Luo GQ (2023). Broadband and compact folded substrate integrated waveguide phase shifter and its application to 180° directional coupler. *International Journal of Microwave and Wireless Technologies* **15**, 554–559. <https://doi.org/10.1017/S1759078722000915>

Received: 8 May 2022
Revised: 14 July 2022
Accepted: 14 July 2022

Key words:

Broadband; compact; complementary splitting resonators (CSRRs); Folded substrate integrated waveguide (FSIW); Phase shifter

Author for correspondence:

Guo Qing Luo,
E-mail: luoqing@hdu.edu.cn

Abstract

In this paper, a broadband, low insertion loss, and compact folded substrate integrated waveguide (FSIW) phase shifter is proposed for the first time. By loading the complementary splitting resonators (CSRRs) on the middle metal layer of the FSIW, a closed-type slow-wave transmission line (TL) is obtained, which can provide a wideband phase shift (39%) compared with the equal-length fast-wave one. The enclosed structure of the CSRR-loaded FSIW prevents the CSRRs from radiation as suffered in the previous reported CSRR-loaded TLs, resulting in a low insertion loss. This feature greatly reduces the amplitude imbalance between the main line and the reference line of the phase shifter. In addition, no transition structure is required between the FSIWs with and without CSRRs for broadband impedance matching, which makes the phase shifter more compact and easier to integrate with other FSIW devices. To validate the performance of the proposed phase shifter and to illustrate its ease integration, a novel FSIW 180° directional coupler that consists of an FSIW 90° coupler and an FSIW 90° phase shifter is designed, fabricated, and measured. The measured results agree well with the simulated data.

Introduction

Substrate integrated waveguide (SIW) has attracted much attention due to its merits of low loss, low cost, low interference, easy fabrication, and planar integration [1]. However, the footprint of the SIW is large. For size reduction, several SIW-derived transmission lines (TLs), including the half-mode SIW (HMSIW) [2], ridge SIW [3], and folded SIW (FSIW) [4, 5], have also been proposed. Based on these structures, a variety of microwave devices, such as bandpass filters [6–8], directional couplers [9, 10], and phase shifters [11–18], have been proposed. To feature as a good phase shifter, it has to show a wide bandwidth, a good impedance matching, a low insertion loss, a compact size, and an equal-length structure.

Traditional SIW phase shifters implemented by delay lines [12] or equal-length unequal-width SIWs [13] are frequency dependent, and therefore, they are narrowband in nature. In [14], a wideband (49%) self-compensating SIW phase shifter is proposed. However, this phase shifter and its reference line show different physical lengths. To achieve a wide bandwidth with an equal-length structure, a dielectric slab [15] or an artificial dielectric slab [16, 17] can be inserted into the SIW. However, a multi-section impedance transformer is required for a wideband impedance matching, resulting in a large circuit size. By etching complementary split-ring resonators (CSRRs) on the cover of SIW or HMSIW, more compact equal-length phase shifters with a wide bandwidth are realized [18]. However, they suffer from a high insertion loss and a large amplitude imbalance caused by the radiation loss of the CSRRs. Therefore, each of the existed SIW phase shifters accomplishes only part of the requirements.

On the other hand, a 180° directional coupler is a key component in many microwave circuits, such as push-pull amplifiers, balanced mixers, and antenna feeding networks. To provide a 180° coupler characteristic, several hybrid ring couplers based on SIW and FSIW techniques have been proposed [19, 20]. However, these structures suffer from a large footprint. Another technique of cascading a 90° directional coupler with a 90° phase shifter to obtain a 180° directional coupler has also been proposed in [21–23]. However, the bandwidth of the 180° directional coupler is limited by the phase shifter.

In this paper, a broadband equal-length CSRR-loaded FSIW phase shifter is proposed for the first time. By loading the CSRRs on the middle metal layer of the FSIW, a closed-type slow-wave TL is obtained, which can provide a wideband phase shift (39%) compared with the equal-length fast-wave one. The enclosed structure of the CSRR-loaded FSIW prevents the CSRRs from radiation as suffered in the CSRR-loaded SIW and HMSIW TLs [18], resulting in a low insertion loss. This feature greatly reduces the amplitude imbalance between the

main line and the reference line of the phase shifter. Thus, the proposed design exhibits a lower insertion loss and a smaller amplitude imbalance as compared with the CSRR-loaded SIW and HMSIW phase shifters in [18]. Furthermore, an FSIW 180° directional coupler that consists of an FSIW 90° coupler and a 90° phase shifter is designed, fabricated, and measured to verify the concept. The proposed FSIW 180° directional coupler exhibits a wide bandwidth while occupies a small circuit size.

FSIW phase shifter

Figure 1 shows the structure of the proposed CSRR-loaded FSIW. It consists of two layers of dielectric substrate, two rows of metallic via-holes, and three metal planes. Both of the substrates are Tanconic TLY-5 with relative dielectric constant $\epsilon_r = 2.2$, loss tangent $\tan\delta = 0.0009$, and thickness $h = 0.508$ mm. The metallic via-holes are connected between the top and bottom metal planes, which are not shown here for better clarity of the interior details. The diameter of the metallic via-holes is $d_v = 0.5$ mm, and the space between two adjacent via-holes is $p_v = 0.9$ mm. The CSRRs are etched on the middle metal plane of the FSIW with a periodical arrangement to implement a slow-wave TL with a closed structure.

To illustrate the slow-wave effect of the CSRR-loaded FSIW, full wave simulations of the proposed structure were carried out by using Ansys high-frequency structure simulator. Figure 2 shows the simulated electric field distributions inside the normal FSIW and the CSRR-loaded FSIW at 13 GHz. For the CSRR-loaded FSIW, typical folded TE₁₀ mode is firstly excited, when it transmits to the CSRR-loaded region, the guided wavelength is reduced, revealing that the phase velocity is slowed down. Therefore, a stable phase shift can be obtained between the equal-length FSIWs with and without CSRRs.

To know in detail how the parameters affect the phase shift performance, a CSRR-loaded FSIW unit cell, as shown in

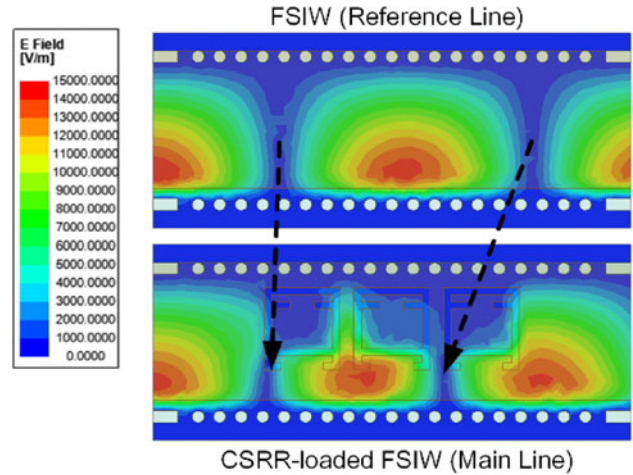


Fig. 2. The E-field distributions inside the normal FSIW and the CSRR-loaded FSIW at 13 GHz.

Fig. 3, is studied. To begin with, the parameters are set as follows: $w = l = 3$, $s = 0.3$, $c = 1.6$, $d = 0.6$, $l_{S1} = l_{S2} = 1.6$, $W_F = 6.3$, and $g = 0.7$ (unit: mm). Figure 4 shows the simulated phase shifts of the unit cell against different values of w , l , s , c , d , and l_{S2} . As can be observed, the phase shift of a unit cell can be varied from 20° to 40° in 10–16 GHz. It increases with the increase of the values of w , l , and d , and decreases with the increase of the values of s , c , and l_{S2} . In addition, the slope of the phase shift can be controlled by modifying the values of l , s , and d . In this way, a flat phase shift over a wide bandwidth can be obtained. The parameter l_{S1} has little influence on the phase shift. It should be mentioned that, in Figs 4(a)–4(g), only one parameter is swept at the same time, while the other parameters are kept unchanged. If two or more parameters (e.g. w and l) are adjusted simultaneously, the phase shift range of the unit cell would be larger than 20–40 degree. Due to the strong loading effect of the CSRR, only countable CSRR-loaded cells are needed to obtain a required phase shift, resulting in a compact size.

To realize a 90° phase shifter, three CSRRs are needed. Figure 5(a) shows the simulated phase shift of the 90° phase shifter, whose dimensions are: $w = 3.15$, $l = 3.5$, $s = 0.3$, $c = 1.7$, $d = 0.8$, $l_{S1} = 1$, $l_{S2} = 1.8$, $p = 0.6$, $W_F = 6.3$, and $g = 0.7$ (unit: mm). As can be observed, a stable phase shift of $90^\circ \pm 5^\circ$ is obtained from

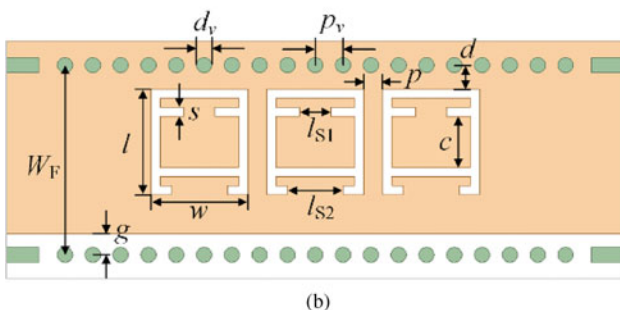
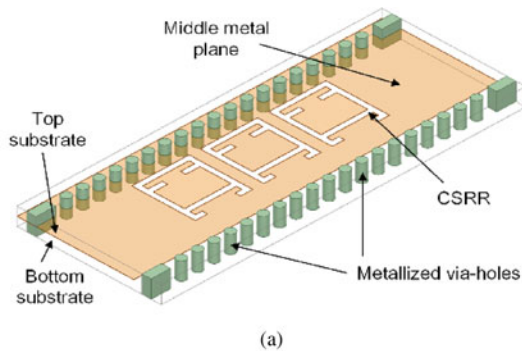


Fig. 1. Configuration of the CSRR-loaded FSIW phase shifter. (a) 3D view. (b) Top view.

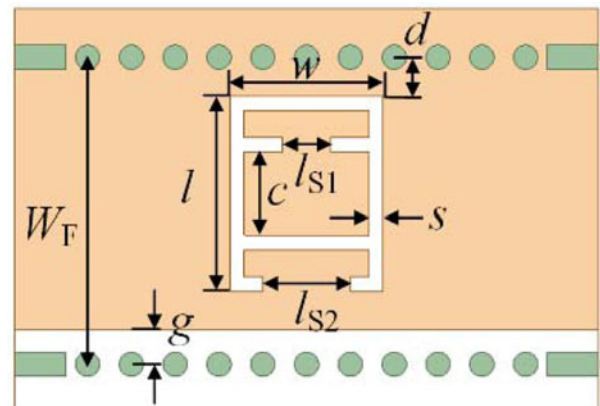


Fig. 3. Layout of the CSRR-loaded FSIW unit cell.

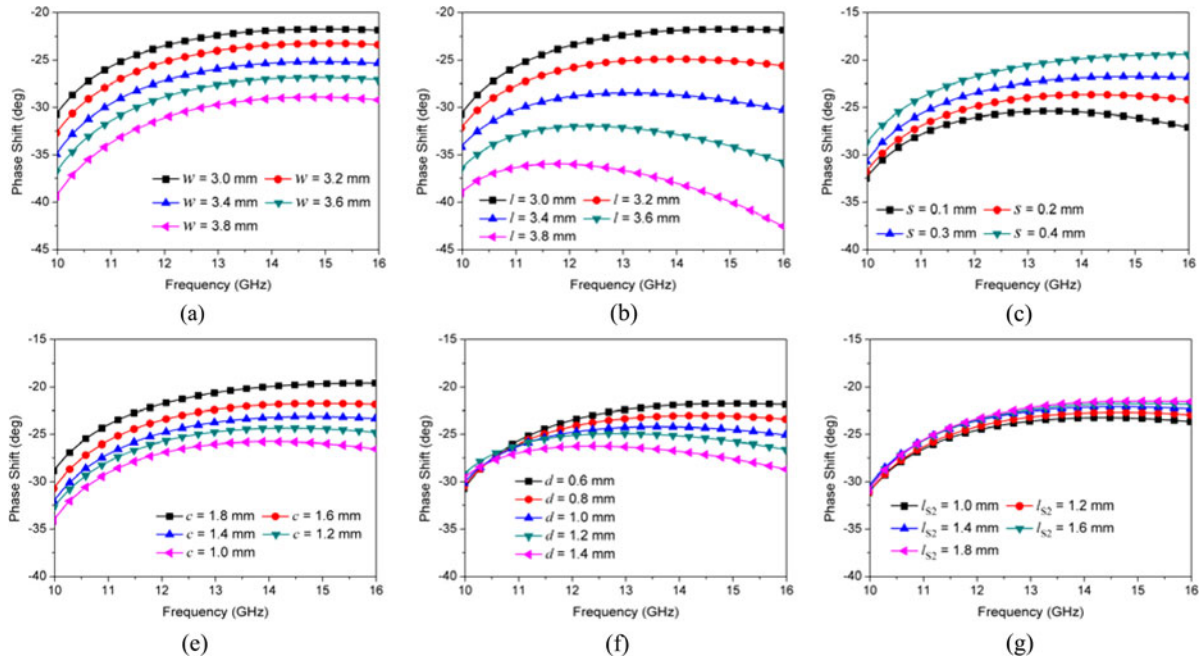


Fig. 4. Simulated phase shifts of a CSRR-loaded unit cell against different values of (a) w , (b) l , (c) s , (d) c , (e) d , and (f) l_{S2} .

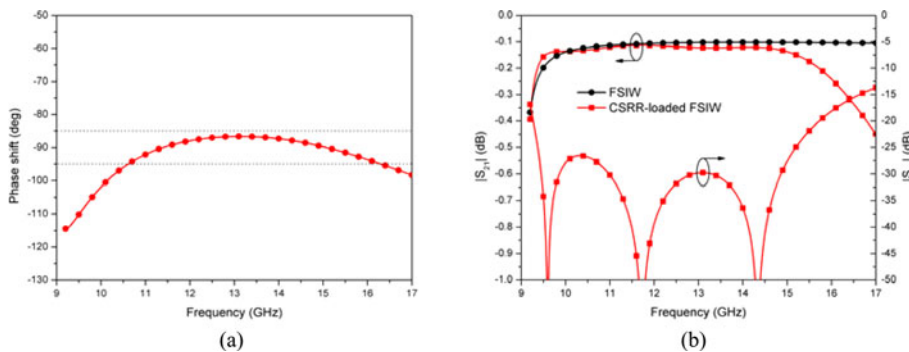


Fig. 5. Simulated results of the 90° phase shifter. (a) Phase shift. (b) S-parameters.

Table 1. Comparison with other broadband phase shifters

Ref.	f_0 (GHz)	FBW (%)	Phase shift (°)	IL (dB)	AI (dB)	EL	Size (λ_g^2)
[14]	32	49	90 ± 2.5	<0.5	<0.2	No	2.2
[16]	26	46	89.5 ± 5	<0.8	<0.1	Yes	2.08
[15]	41	39	92 ± 4	≈ 0.2	N/A	Yes	3.04
[18]-I	8.5	35	90 ± 5	<0.7	<0.55	Yes	0.67
[18]-II	8.5	35	91 ± 4.5	<0.9	N/A	Yes	0.37
This work	13.15	39	90 ± 5	<0.2	<0.1	Yes	0.28

f_0 , center frequency; AI, amplitude imbalance; EL, equal length for reference and main lines; λ_g , wavelength in the dielectric substrate at f_0 .

10.6 to 16.3 GHz. Figure 5(b) shows the simulated $|S_{21}|$ and $|S_{11}|$ of the CSRR-loaded FSIW (i.e. the main line) and the simulated $|S_{21}|$ of the normal FSIW (i.e. the reference line). From 10.6 to 15.7 GHz, the insertion losses of both the main line and the reference line are lower than 0.2 dB, and the amplitude imbalance between them is less than 0.1 dB. The simulated return loss ($|S_{11}|$) of the CSRR-loaded FSIW is better than 20 dB from 10.6 to 15.7 GHz

without using any transition structures. This makes the proposed phase shifter more compact and easier to integrate with other devices. The core size of the FSIW 90° phase shifter is 10.65 mm × 6.3 mm, excluding the input and output FSIW sections.

Table 1 summarized a comparison between the proposed FSIW phase shifter and other existing SIW and HMSIW phase shifters. Compared with the phase shifters in [14–16], the

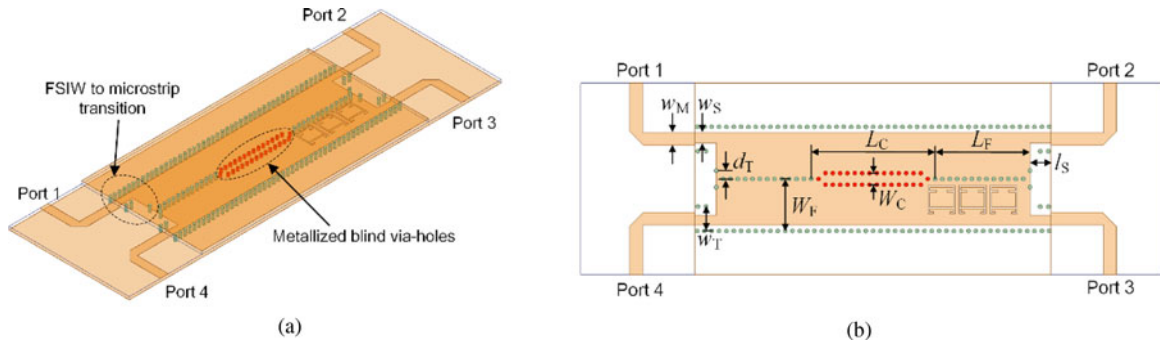


Fig. 6. Configuration of the FSIW 180° coupler. (a) 3D view. (b) Top view.

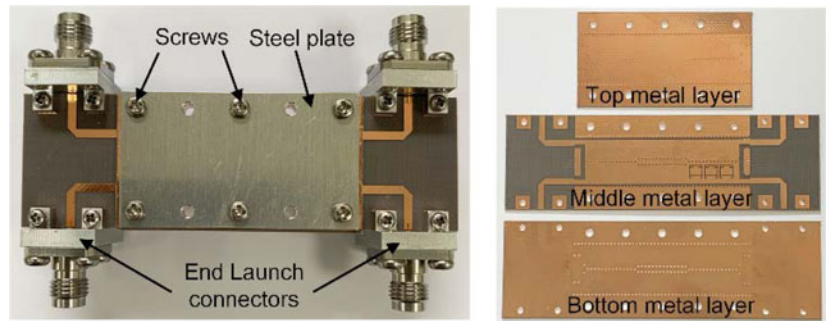


Fig. 7. Photograph of the fabricated FSIW 180° coupler.

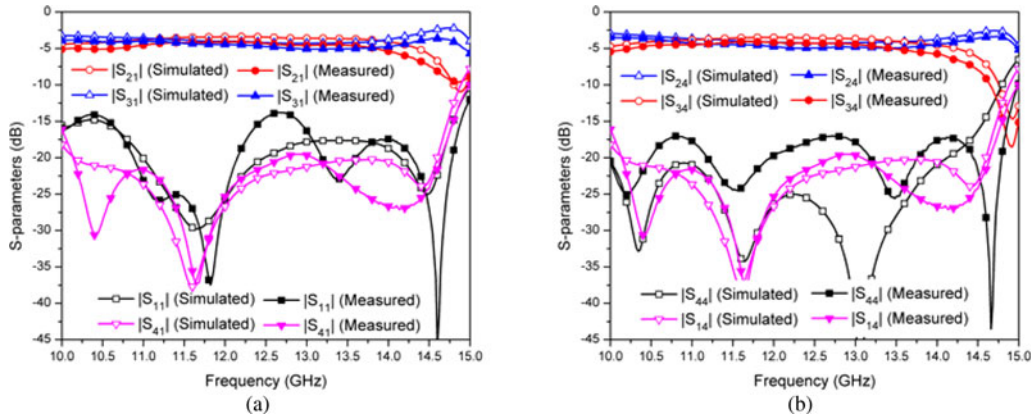


Fig. 8. Simulated and measured S-parameters of the proposed 180° coupler. (a) Excited at port 1. (b) Excited at port 4.

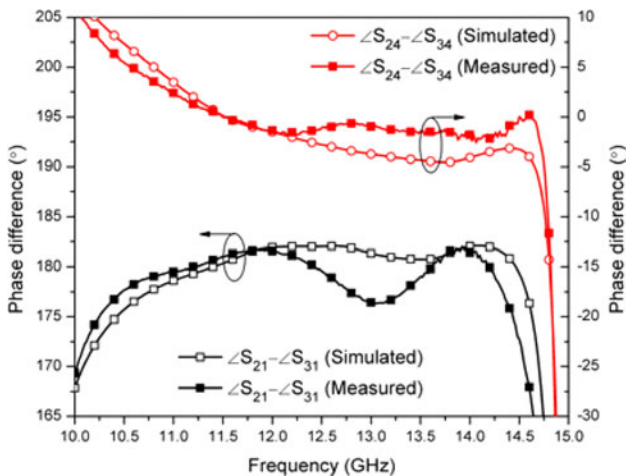


Fig. 9. Simulated and measured phase difference between port 2 and port 3 of the proposed 180° coupler.

proposed design achieves a more compact size. Compared with the CSRR-loaded SIW and HMSIW phase shifters [18], the proposed design exhibits a lower insertion loss and a smaller amplitude imbalance, thanks to the closed structure. It should be mentioned that the size reduction of the proposed phase shifter is not only contributed by the folded structure, but also contributed by the slow-wave effect and the non-transition structure. Therefore, the size of the proposed FSIW phase shifter is smaller than 50% of the SIW counterparts.

FSIW 180° directional coupler

To validate the performance of the proposed phase shifter and to illustrate its ease integration, an FSIW 180° directional coupler that consists of an FSIW 90° coupler [24] and an FSIW 90° phase shifter is designed, fabricated, and measured. The structure of the 180° directional coupler is shown in Fig. 6, and the detailed

Table 2. Comparison with other 180° couplers

Ref.	[19]	[20]	[21]	[22]	[23]	This work
f_0 (GHz)	27	28.2	11	36	35	12.05
FBW	7%	4.3%	15.5%	6.1%	17%	26%
Techn.	SIW	FSIW	HMSIW	SIW	SIW	FSIW
AI (dB)	± 0.25	± 0.3	± 0.25	± 0.25	± 0.6	± 0.5
PI (°)	N/A	± 10	± 10	± 5	± 10	± 5
Isolation (dB)	>25	>20	>19	>19.2	>14	>19.2
Size (λ_g^2)	9.84	7.54	2.65*	3.85*	1.62*	1.2*

*The length of the coupler is calculated by adding the length of the coupling region and the length of the phase shifter; f_0 , center frequency; λ_g , wavelength in the dielectric substrate at f_0 ; AI, amplitude imbalance; PI, phase imbalance.

dimensions are $W_F = 6.3$, $L_F = 11.65$, $W_C = 1.4$, $L_C = 15.2$, $d_T = 0.85$, $l_S = 2.6$, $w_T = 2.95$, $w_S = 1.2$, $w_M = 1.55$, $g = 0.7$, $w = 3.3$, $l = 3.4$, $s = 0.2$, $l_{S1} = 1.3$, $l_{S2} = 2$, $p = 0.5$, $c = 1.8$, $d = 0.8$ (unit: mm).

By adjusting the length L_C of the coupling region and the distance W_C of the two rows of metallized blind via-holes (red ones) on the bottom substrate, a flat 90° phase difference with a stable power ratio can be obtained [24]. The CSRR-loaded phase shifter is used to provide another 90° phase shift. A broadband microstrip to FSIW transition [25] is used for measurement.

The photograph of the fabricated FSIW 180° coupler is shown in Fig. 7. The PCB processing technology is used for layered processing. Considering the integration of the whole structure, two steel plates are added to the upper and lower surfaces of the coupler, and the double layers are manually tightened with screws. The core size of the proposed 180° coupler is 26.85 mm × 12.6 mm, where the length is calculated by adding the length of the coupling region (L_C) and the length of the phase shifter (L_F). The fabricated 180° coupler is measured by using a Keysight N5234B vector network analyzer, two ports at a time, with the unused ports terminated in a 50 Ω loads.

Figure 8 shows the simulated and measured S-parameters of the FSIW 180° coupler. When the coupler is excited at port 1, the measured $|S_{11}|$ is better than 13.8 dB from 10 to 14.8 GHz, and the measured $|S_{21}|$ and $|S_{31}|$ are -4.5 ± 0.5 dB in 10.5–13.9 GHz with a fractional bandwidth (FBW) of 28%. When the coupler is excited at port 4, the measured $|S_{44}|$ is better than 17 dB from 10 to 14.8 GHz, and the measured $|S_{24}|$ and $|S_{34}|$ are -4.6 ± 0.5 dB in 10.5–13.6 GHz with an FBW of 26%. The measured isolation between port 1 and port 4 is better than 19.5 dB from 10.1 to 14.6 GHz. Considering the insertion losses of the End Launch connectors, the measured results are in accordance with the simulated data.

Figure 9 shows the simulated and measured phase difference between port 2 and port 3 under different scenarios. The measured phase difference is $180^\circ \pm 5^\circ$ from 10.3 to 14.4 GHz for an excitation of port 1 and $0^\circ \pm 5^\circ$ from 10.5 to 14.7 GHz for an excitation of port 4, which are consistent with the simulated ones.

Table 2 summarized a comparison between the proposed 180° directional coupler and other 180° directional couplers. The proposed 180° directional coupler exhibits the widest bandwidth while occupies the smallest circuit size.

Conclusion

In this paper, a CSRR-loaded FSIW phase shifter and its application to a 180° directional coupler is presented. By loading the

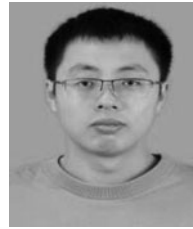
CSRRs on the middle metal layer of the FSIW, a broadband (39%), low insertion loss (<0.2 dB), and compact equal-length phase shifter is obtained. Compared with the SIW and HMSIW counterparts, the proposed phase shifter exhibits a lower insertion loss and a lower amplitude imbalance. To validate the concept, an FSIW 180° directional coupler that consists of an FSIW 90° coupler and an FSIW 90° phase shifter is designed, fabricated, and measured. Good agreement between the simulated and measured results is obtained.

Acknowledgement. This work was supported in part by the “Pioneer” and “Leading Goose” R&D Program of Zhejiang under Grant 2022C01119 and in part by the Natural Science Foundation of China under Grant 61901147 and 62125105.

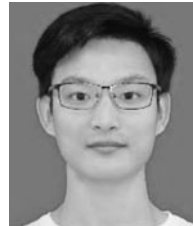
References

1. **Bozzi M, Georgiadis A and Wu K** (2011) Review of substrate-integrated waveguide circuits and antennas. *IET Microwaves, Antennas & Propagation* **5**, 909–920.
2. **Lai Q, Fumeaux C, Hong W and Vahldieck R** (2009) Characterization of the propagation properties of the half-mode substrate integrated waveguide. *IEEE Transactions on Microwave Theory and Techniques* **57**, 1996–2004.
3. **Bozzi M, Winkler SA and Wu K** (2010) Broadband and compact ridge substrate-integrated waveguides. *IET Microwaves, Antennas & Propagation* **4**, 1965–1973.
4. **Grigoropoulos N, Sanz-Izquierdo B and Young PR** (2005) Substrate integrated folded waveguides (SIFW) and filters. *IEEE Microwave and Wireless Components Letters* **15**, 829–831.
5. **Che W, Geng L, Deng K and Chow YL** (2008) Analysis and experiments of compact folded substrate-integrated waveguide. *IEEE Transactions on Microwave Theory and Techniques* **56**, 88–93.
6. **Macchiarella G, Tomassoni C and Bozzi M** (2022) Compact SIW filters with transmission zeros: a review and current trends. *International Journal of Microwave and Wireless Technologies* **14**, 336–344.
7. **Liu Q, Zhou D, Zhang D, Bian C and Zhang Y** (2020) Ultra-compact quasi-elliptic bandpass filter based on capacitive-loaded eighth-mode SIW cavities. *International Journal of Microwave and Wireless Technologies* **12**, 109–115.
8. **Zhu F, Luo GQ, You B, Zhang XH and Wu K** (2021) Planar dual-mode bandpass filters using perturbed substrate-integrated waveguide rectangular cavities. *IEEE Transactions on Microwave Theory and Techniques* **69**, 3048–3057.
9. **Ho M-H, Hong Y-H and Li J-C** (2018) Novel rat-race coupler design of arbitrary coupling coefficient using substrate integrated waveguide cavity. *International Journal of Microwave and Wireless Technologies* **10**, 861–869.

10. **Bayati MS and Khorand T** (2020) Compact SIW directional filter using substrate integrated circular cavities. *International Journal of Microwave and Wireless Technologies* **12**, 352–355.
11. **Cheng X, Yao Y, Tomura T, Hirokawa J, Yu T, Yu J and Chen X** (2018) Millimeter-wave frequency beam scanning array with a phase shifter based on substrate-integrated-waveguide. *IEEE Access* **6**, 47408–47414.
12. **Xu X, Bosisio RG and Wu K** (2005) A new six-port junction based on substrate integrated waveguide technology. *IEEE Transactions on Microwave Theory and Techniques* **53**, 2267–2273.
13. **Cheng Y, Hong W and Wu K** (2007) “Novel substrate integrated waveguide fixed phase shifter for 180-degree direction coupler,” in IEEE MTT-S International Microwave Symposium Digest, pp. 189–192.
14. **Cheng YJ, Hong W and Wu K** (2010) Broadband self-compensating phase shifter combing delay line and equal-length unequal-width phaser. *IEEE Transactions on Microwave Theory and Techniques* **58**, 203–210.
15. **Cano JL, Villa E, Mediavilla A and Artal E** (2018) A wideband correlation and detection module based on substrate-integrated waveguide technology for radio astronomy applications. *IEEE Transactions on Microwave Theory and Techniques* **66**, 3145–3152.
16. **Djerafi T, Wu K and Tatu SO** (2015) Substrate-integrated waveguide phase shifter with rod-loaded artificial dielectric slab. *Electronics Letters* **51**, 707–709.
17. **Boudreau I, Wu K and Deslandes D** (2011) “Broadband phase shifter using air holes in Substrate Integrated Waveguide,” in IEEE MTT-S International Microwave Symposium Digest, Baltimore, MD, USA, pp. 1–4.
18. **Liu S and Xu F** (2019) Novel substrate-integrated waveguide phase shifter and its application to six-port junction. *IEEE Transactions on Microwave Theory and Techniques* **67**, 4167–4174.
19. **Che W, Deng K, Yung KN and Wu K** (2006) H-plane 3 dB hybrid ring of high isolation in substrate integrated rectangular waveguide (SIRW). *Microwave and Optical Technology Letters* **48**, 502–505.
20. **Ding Y and Wu K** (2009) “Miniaturized hybrid ring circuits using T-type folded substrate integrated waveguide (TFSIW),” in IEEE MTT-S International Digest, pp. 705–708.
21. **Liu B, Hong W, Zhang Y, Tang H-J, Yin X and Wu K** (2007) Half mode substrate integrated waveguide 180° 3-dB directional couplers. *IEEE Transactions on Microwave Theory and Techniques* **55**, 2586–2592.
22. **Cheng YJ, Hong W and Wu K** (2008) Design of a monopulse antenna using a dual V-type linearly tapered slot antenna (DVL TSA). *IEEE Transactions on Antennas and Propagation* **56**, 2903–2909.
23. **Li A and Luk K-M** (2019) Millimeter-wave dual linearly polarized endfire antenna fed by 180° hybrid coupler. *IEEE Antennas and Wireless Propagation Letters* **18**, 1390–1394.
24. **Sun Q, Ban Y-L, Lian J-W, Liu Y and Nie Z** (2020) Millimeter-wave multibeam antenna based on folded C-type SIW. *IEEE Transactions on Antennas and Propagation* **68**, 3465–3476.
25. **Xu J, Xu F and Li D** (2015) “A planar magic-T based on folded substrate integrated waveguide”, in Proceedings of Asia-Pacific Microwave Conference (APMC), pp. 1–3.



Xin Zhao received the B.S. degree from the Nanjing University of Posts and Telecommunications, Nanjing, China, in 2017. He is currently pursuing the M.S. degree with Hangzhou Dianzi University, Hangzhou, China. His current research interests include microwave and millimeter-wave integrated circuits and high-performance passive components.



Junhao Sheng received the B.S. degree in electronic science and technology from Hunan City University, Yiyang, China in 2019. He is currently pursuing the M.S. degree with Hangzhou Dianzi University, Hangzhou, China. His current research interests include microwave and millimeter-wave integrated circuits and high-performance passive components.



Guo Qing Luo received the B.S. degree from the China University of Geosciences, Wuhan, China, in 2000, the M.S. degree from Northwest Polytechnical University, Xi'an, China, in 2003, and the Ph.D. degree from Southeast University, Nanjing, China, in 2007. Since 2007, he has been a Lecturer with the Faculty of School of Electronics and Information, Hangzhou Dianzi University, Hangzhou, China, and was promoted to Professor in 2011. From October 2013 to October 2014, he joined the Department of Electrical, Electronic and Computer Engineering, Heriot-Watt University, Edinburgh, UK, as a Research Associate, where he was involved in developing low-profile antennas for UAV applications. He has authored or co-authored over 110 technical papers in refereed journals and conferences and holds 19 patents. His current research interests include RF, microwave and mm-wave passive devices, antennas, and frequency-selective surfaces.



Fang Zhu received the B.S. degree in electronics and information engineering from Hangzhou Dianzi University, Hangzhou, China, in 2009, and the M.S. and Ph.D. degrees in electromagnetic field and microwave technique from Southeast University, Nanjing, China, in 2011 and 2014, respectively. From 2014 to 2016, he was a MMIC Designer with Nanjing Millway Microelectronics Technology Co., Ltd, Nanjing, China. From 2016 to 2019, he was a Postdoctoral Research Fellow with the Poly-Grames Research Center, Polytechnique Montréal, Montréal, QC, Canada. He is currently a Professor with the School of Electronics and Information, Hangzhou Dianzi University, Hangzhou, China. His current research interests include microwave and millimeter-wave integrated circuits, components, and transceivers for wireless communication and sensing systems.